Bull. Chem. Soc. Jpn., 70, 1077—1083 (1997)

Cooperative Redox Regulation of [4Fe-4S] Ferredoxin Model Arenethiolate Complexes by NH···S Hydrogen Bonds and an Aromatic C–H···S Interaction

Takafumi Ueno, Masahiro Inohara, Norikazu Ueyama, and Akira Nakamura*

Department of Macromolecular Science, Graduate School of Science, Osaka University, Toyonaka, Osaka 560

(Received November 21, 1996)

A series of the model complexes containing *ortho*-substituted arenethiolato ligands, $((Et_4N)_2[Fe_4S_4(S\text{-}2\text{-}RCONHC_6H_4)_4]$ {R = Ph (**1**), 4-MeO–C_6H_4 (**2**), and 4-F–C_6H_4 (**3**)} and $(Et_4N)_2[Fe_4S_4\{S\text{-}2,6\text{-}(RCONH)_2C_6H_3\}_4]$ {R = Ph (**4**), 4-MeO–C_6H_4 (**5**), and 4-F–C_6H_4 (**6**)}) was synthesized and characterized by ^{1}H NMR, IR spectroscopy, and cyclic voltammetry. The solution structures of these complexes are discussed based on their ^{1}H NMR T_1 data and molecular-dynamics calculations. Complex **4** has a shorter distance (av. 4.3 Å) between the protons of the benzoyl group and the inorganic sulfur atom of the [4Fe-4S] cluster than the corresponding ones of **1** (av. 6.2 Å). These results indicate the C–H···S interaction between the protons of the benzoyl group and the sulfur atom of the [4Fe-4S] cluster. The $[Fe_4S_4(SAr)_4]^{2-}/[Fe_4S_4(SAr)_4]^{3-}$ redox potential for **1** and **4** are −0.86 and −0.65 V, respectively. The difference between **1** and **4** is Δ0.21 V. This is larger than the value Δ0.11 V between $[Fe_4S_4(S\text{-}2\text{-}t\text{-}BuCONHC_6H_4)_4]^{2-}$ (−0.91 V) and $[Fe_4S_4\{S\text{-}2,6\text{-}(t\text{-}BuCONH)_2C_6H_3\}_4]^{2-}$ (−0.80 V), considered to be the difference between singly and doubly NH···S hydrogen-bonded complexes. The redox potentials for **1**—**6** follow the trend of the Hammett σ_m values, showing that the aromatic ring of the benzoyl group interacts with the [4Fe-4S] cluster directly. A cooperative effect between the C–H···S interaction and the NH···S hydrogen bond is thus found to regulate the redox potential of the model complexes.

To elucidate the regulation of the activity of iron–sulfur clusters by the unique microstructure of the environment in native proteins, extensive studies were made for model complexes,[1] native and mutant proteins.[2] Among iron–sulfur proteins, ferredoxins (Fds) and high-potential iron–sulfur proteins (HiPIPs) have [4Fe-4S] clusters coordinated with four cysteinyl sulfur ligands at their active sites. Upon electron transfer, Fds utilize the redox couple of $[Fe_4S_4(SR)_4]^{3-}/[Fe_4S_4(SR)_4]^{2-}$ and HiPIPs use $[Fe_4S_4(SR)_4]^{2-}/[Fe_4S_4(SR)_4]^{1-}$. The correlation between the micro-environments of such [4Fe-4S] clusters and their electron-transfer functions still remains ambiguous. Among possible causes, an important role of the NH···S hydrogen bond has been reported.[3—6]

From an X-ray structural analysis of *B. thermoproteolyticus* and *P. aerogenes* Fd, a Tyr residue and eight NH···S hydrogen bonds have been reported to be conserved around a [4Fe–4S] cluster.[7] On the other hand, HiPIPs have four or more aromatic residues and five NH···S hydrogen bonds around a [4Fe–4S] cluster in the crystal structures of *R. tenius, E. halophila*, and *C. vinosum* HiPIPs.[8]

One of the chemical functions of the aromatic rings has been thought to be the construction of a hydrophobic domain and support of the NH···S hydrogen bond. The effect of the NH···S hydrogen bond on the redox potential was studied by using ferredoxin peptide model complexes[6,9] or various simple 2-mono- and 2,6-bis(acylamino)benzenethiolate model complexes.[4] Chemically designed [4Fe-4S] ferredoxin model complexes having adjacent aromatic rings have been synthesized as models of chemical simulation of the environments of aromatic rings around a [4Fe-4S] cluster.[10,11]

In native systems, an interaction between aromatic residues and sulfur atoms has been proposed based on a ^{1}H NMR investigation of *E. halophila* and *E. vacuolata* HiPIPs.[12] In addition, the direct interaction of an aromatic ring with the Fe–S cluster in mutant *C. vinosum* HiPIP has been shown by ^{19}F NMR spectroscopy.[13] The importance of the chemical functions of the aromatic ring on the redox property still remains obscure and needs to be studied.

Recently, it have been suggested that the number and orientations of aromatic rings around the [4Fe–4S] cluster contribute to the modulation of redox reactions.[8] Our previous study suggested that the coexistence of aromatic ring and NH···S hydrogen bond contributes to the stabilization of the $[Fe_4S_4(SAr)_4]^{2-}/[Fe_4S_4(SAr)_4]^{1-}$ redox couple when Ar is 2-*t*-BuCONH-6-PhC_6H_3.[14] In this case, the conformer with aromatic ring stacking over the thiolate sulfur atom is illustrated in Fig. 1a.[15]

The existence of a sulfur-aromatic interaction has already been suggested by Reid et al.[16] They documented a statistically significant preferred separation distance of < 6 Å between the sulfur atom and the ring centroid. In addition, the angle between the sulfur atom and the ring plane is preferred to be at 0—30° and ca. 45°. Two ranges of the angle mean the existence of distinct interactions. The sulfur–aromatic interaction is presumed to occur through a C–H···S

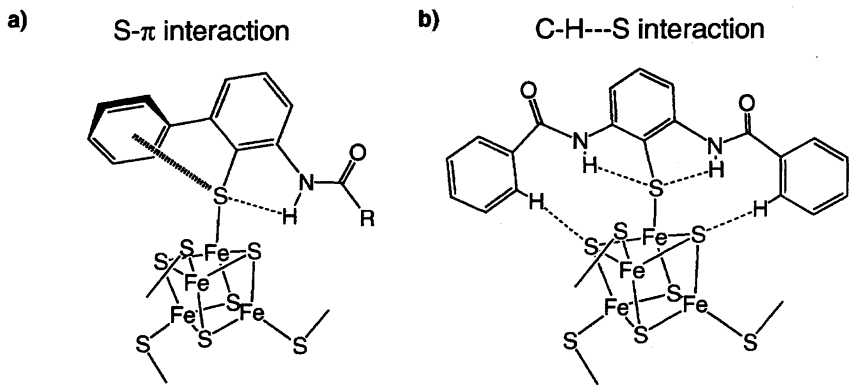

Fig. 1. Schematic drawing of model complexes designed for realizing two different sulfur–aromatic interactions; a) S–π interaction and b) C–H···S interaction.

interaction between a negatively charged sulfur atom and a positively charged hydrogen atom of the ring with an angle of 0—30°.[16] This interaction is caused by an S–π interaction between a sulfur p orbital and a π orbital of the ring with an angle of ca. 45°.[15] It is believed that these interactions contribute to the stabilization of protein folding.[15,16]

In this paper we report on the cooperative effect of the neighboring aromatic rings and double NH···S hydrogen bonds on the electrochemical property of the [4Fe-4S] cluster using a newly designed arenethiolate ligands, 2,6-$(PhCONH)_2C_6H_3S^-$. The aromatic ring of the benzoyl group can preferentially interact with the inorganic sulfur atom, because the ring maintains coplanarity with the amide and arenethiolate groups (Fig. 1b).

Results and Discussion

Detection of NH···S Hydrogen Bond. The IR spectra of the complexes were measured in the solid state in order to detect the presence of a NH···S hydrogen bond. Table 1 gives selected IR bands in the amide region of $[Fe_4S_4(SAr)_4]^{2-}$ and the corresponding organic disulfides. The *ortho*-substituted complex, $[Fe_4S_4(S\text{-}2\text{-}PhCONHC_6H_4)_4]^{2-}$ (**1**), containing a single NH···S hydrogen bond, exhibits a NH band at 3296 cm^{-1} and a C=O band at 1660 cm^{-1}. The differences, $\Delta\nu$(NH) and $\Delta\nu$(C=O), between **1** and the corresponding disulfide, $(2\text{-}PhCONHC_6H_4S)_2$, were estimated to be 79 and 15 cm^{-1}, respectively, when the band for the corresponding disulfide was employed as a standard. Similar $\Delta\nu$(NH) values have been observed for various single NH···S hydrogen-bonded metal complexes, e.g. 75 cm^{-1} for $[Fe_4S_4(S\text{-}2\text{-}t\text{-}BuCONHC_6H_4)]^{2-}$[4] and 59 cm^{-1} for $[Mo^{IV}(S\text{-}2\text{-}t\text{-}BuCONHC_6H_4)_4]^{2-}$[5] These results indicate the presence of a NH···S hydrogen bond in **1**. The $\Delta\nu$(NH) (76 cm^{-1}) and $\Delta\nu$(C=O) (11 cm^{-1}) of a *p*-fluoro derivative, $[Fe_4S_4\{S\text{-}2\text{-}(4\text{-}F\text{-}C_6H_4CONH)C_6H_4\}_4]^{2-}$ (**3**), have similar values to $[Fe_4S_4(S\text{-}2\text{-}t\text{-}BuCONHC_6H_4)]^{2-}$.[4] Therefore, **3** has an intramolecular NH···S hydrogen bond in the solid state. The *p*-methoxy analog, $[Fe_4S_4\{S\text{-}2\text{-}(4\text{-}MeO\text{-}C_6H_4CONH)\text{-}C_6H_4\}_4]^{2-}$ (**2**), shows negative values for $\Delta\nu$(NH) of −27 cm^{-1} and $\Delta\nu$(C=O) of −18 cm^{-1} (Table 1). The reason for the negative shifts of **2** is that the values of the corresponding disulfide, $\{2\text{-}(4\text{-}MeO\text{-}C_6H_4CONH)C_6H_4S\}_2$, have ν(NH) at 3726 cm^{-1} and ν(C=O) at 1645 cm^{-1}, assignable to intermoleculary hydrogen-bonded NH and CO bands, respectively, as observed for $(2\text{-}t\text{-}BuCONHC_6H_4S)_2$.[17] The presence of an intramolecular NH···S hydrogen bond in **2** has been confirmed by a positive shift in its 2−/3− redox potential in acetonitrile (described below).

The 2,6-disubstituted complex $[Fe_4S_4\{S\text{-}2,6\text{-}(PhCONH)_2\text{-}C_6H_3\}_4]^{2-}$ (**4**), containing double NH···S hydrogen bonds, exhibits a $\Delta\nu$(NH) of 90 cm^{-1} and $\Delta\nu$(C=O) of 21 cm^{-1}, as calculated from the amide bands of $\{2,6\text{-}(PhCONH)_2C_6H_3S\}_2$. The *p*-methoxy analog, $[Fe_4S_4\{S\text{-}2,6\text{-}(4\text{-}MeOC_6H_4CONH)_2C_6H_3\}_4]^{2-}$ (**5**) indicates a $\Delta\nu$(NH) of 63 cm^{-1} and a $\Delta\nu$(C=O) of 16 cm^{-1}. $[Fe_4S_4\{S\text{-}2,6\text{-}(4\text{-}F\text{-}C_6H_4CONH)_2C_6H_3\}_4]^{2-}$ (**6**) shows a $\Delta\nu$(NH) of 92 cm^{-1} and a $\Delta\nu$(C=O) of 11 cm^{-1}. These values are similar to the $\Delta\nu$(NH) (63 cm^{-1}) and $\Delta\nu$(C=O) of (21 cm^{-1}) of $(Et_4N)_2[Fe_4S_4\{S\text{-}2,6\text{-}(t\text{-}BuCONH)_2C_6H_3\}_4]$, having a double NH···S hydrogen bond.[4] Therefore, complexes, **4**, **5**, and **6** have an intramolecular double NH···S hydrogen bond.

Solution Structure of $[Fe_4S_4(S\text{-}2\text{-}PhCONHC_6H_4)_4]^{2-}$ (1) and $[Fe_4S_4\{S\text{-}2,6\text{-}(PhCONH)_2C_6H_3\}_4]^{2-}$ (4) Determined from a ^{1}H NMR T_1 Analysis in Acetonitrile. Table 2 summarizes the paramagnetic isotropic shifts for these complexes. The shift of the 3-, 4-, 5-, and 6-proton signals is essentially similar to those of the known ferredoxin model complexes with *p*-substituted benzenethiolato ligands.[11] The observed shift values of the NH···S hydrogen-bonded NH signal for **1** and **4** are 0.15 and −0.01 ppm, respectively. Such slight isotropic shifts have already been observed for $[Fe_4S_4\{S\text{-}2,6\text{-}(t\text{-}BuCONH)_2C_6H_3\}]^{2-}$[4] and various [4Fe-4S] peptide model complexes.[9] The isotropic shifts of benzoyl 2′, 6′H and 3′, 5′H are 0.39 and 0.05 ppm for **1** and 0.15 and −0.22 for **4**, respectively. The isotropic shifts of benzoyl protons may be caused as a consequence of the [4Fe-4S] cluster, as observed for aromatic protons in $[Fe_4S_4(m\text{-}xyl\text{-}S_2)_2]^{2-}$.[11]

Attempts to analyze the crystal structures of these complexes have been unsuccessful. Therefore, we used a ^{1}H NMR analysis and molecular-dynamics calculations to obtain information about the structures of **1** and **4** in acetonitrile. The relaxation times given in Table 3 were obtained from nonselective inversion-recovery experiments for **1** and

Table 1. Selected IR Bands of $[Fe_4S_4(SAr)_4]^{2-}$ and the Corresponding Disulfide Ar_2S_2 in the Solid State

Ar	ν(NH)/cm^{-1}	$\Delta\nu$(NH)[b]	ν(C=O)/cm^{-1}	$\Delta\nu$(C=O)[b]
2-PhCONHC$_6$H$_4$ (**1**)	3296 (3375)[a]	79	1660 (1675)[a]	15
2-(4-MeO-C$_6$H$_4$CONH)C$_6$H$_4$ (**2**)	3303 (3276)[c]	−27	1662 (1645)[c]	−17
2-(4-F-C$_6$H$_4$CONH)C$_6$H$_4$ (**3**)	3302 (3378)	76	1668 (1679)	11
2,6-(PhCONH)$_2$C$_6$H$_3$ (**4**)	3322 (3412)	90	1669 (1690)	21
2,6-(4-MeO-C$_6$H$_4$CONH)$_2$C$_6$H$_3$ (**5**)	3323 (3386)	63	1665 (1681)	16
2,6-(4-F-C$_6$H$_4$CONH)$_2$C$_6$H$_3$ (**6**)	3323 (3415)	92	1670 (1695)	25
2-*t*-BuCONHC$_6$H$_4$[d]	3314 (3389)	75	1670 (1679)	9
2,6-(*t*-BuCONH)$_2$C$_6$H$_3$[d]	3335 (3398)	63	1674 (1695)	21
2-*t*-BuCONH-6-PhC$_6$H$_3$[e]	3314 (3412)	114	1663 (1690)	27

a) The value in parenthesis refers to the amide NH or CO bond of the corresponding disulfide. b) $\Delta\nu = \nu$(disulfide) − ν(Fe_4S_4 complex). c) The low wavenumbers of NH and CO bands for the disulfide are caused by intermolecular NH···O=C hydrogen bond. d) Ref. 4. e) Ref. 14.

Table 2. ^{1}H Isotropic Shifts of $[Fe_4S_4(SAr)_4]^{2-}$ in Acetonitrile-d_3 at 30 °C

	$(\Delta H/H_0)_{iso}$[a] ppm							
Ar	NH	3H	4H	5H	6H	2′, 6′H	3′, 5′H	
2-PhCONHC$_6$H$_4$ (**1**)	0.15	1.39	−1.47	0.75	−1.18	0.39	0.05	4′H
	(8.98)[b]	(9.43)	(5.83)	(7.81)	(6.41)	(8.04)	(7.49)	−0.06
								(7.49)
2-(4-MeO-C$_6$H$_4$CONH)C$_6$H$_4$ (**2**)	0.29	1.38	−1.44	0.78	−1.16	0.42	0.07	–OMe
	(9.03)	(9.43)	(5.86)	(7.83)	(6.43)	(8.06)	(7.04)	−0.08
								(3.79)
2-(4-F-C$_6$H$_4$CONH)C$_6$H$_4$ (**3**)	0.29	1.43	−1.40	0.77	−1.14	0.41	0.04	
	(9.05)	(9.41)	(5.89)	(7.84)	(6.47)	(8.10)	(7.23)	
2,6-(PhCONH)$_2$C$_6$H$_3$ (**4**)	−0.01	1.23	−0.94	—[c]	—	0.15	−0.22	4′H
	(8.97)	(9.14)	(6.14)			(7.87)	(7.26)	−0.24
								(7.26)
2,6-(4-MeO-C$_6$H$_4$CONH)$_2$C$_6$H$_3$ (**5**)	0	1.16	−1.08	—[c]	—	0.30	−0.07	–OMe
	(8.90)	(9.06)	(6.14)			(8.02)	(6.93)	−0.15
								(3.70)
2,6-(4-F-C$_6$H$_4$CONH)$_2$C$_6$H$_3$ (**6**)	+0.03	1.24	−0.95	—[c]	—	0.09	−0.22	
	(8.93)	(9.10)	(6.28)			(7.88)	(7.01)	

a) $(\Delta H/H_0)_{iso} = (\Delta H/H_0)_{obs} - (\Delta H/H_0)_{dia}$: diamagnetic references are the corresponding disulfides in acetonitrile-d_3 at 30 °C. b) Chemical shifts for $[Fe_4S_4(SAr)_4]^{2-}$ in acetonitrile-d_3 at 30 °C. c) The chemical shift is the same as 3H.

Table 3. T_1 Values (ms) and Calculated Fe···H Distance (Å) of $[Fe_4S_4(SAr)_4]^{2-}$ in Acetonitrile at 30 °C

	2-PhCONHC$_6$H$_4$ (**1**)			2,6-(PhCONH)$_2$C$_6$H$_3$ (**4**)		
	T_1/ms	d_{T1}/Å	d_{MD}/Å	T_1/ms	d_{T1}/Å	d_{MD}/Å
NH	3	3.5	4.2	3	3.5	3.3
2′, 6′H[a]	22	4.9	7.0	15	4.6	5.4
3′, 5′H	84	6.1	8.6	52	5.6	6.5
4′H	200	7.0	9.4	130	6.5	7.0
3H	90	6.1	6.1	50	5.6	5.7
4H	130	6.5	6.3	110	6.4	6.4
5H	60	5.7	5.0	—	—	—
6H	3	3.5	3.0	—	—	—

a) Assigned ^{1}H shown in Fig. 2.

4. In paramagnetic metal complexes the T_1 values are mainly subject to a dipole–dipole interaction. Thus, the metal-proton distances (r_{M-H}) can be correlated to the proton relaxation rates according to the Solomon equation (Eq. 1),[18]

$$T_1^{-1} = C[S(S+1)]r_{M-H}^{-6} f(\tau_c, \omega), \quad (1)$$

where C is a physical constant and $f(\tau_c, \omega)$ is the correlation function. Therefore, the T_1 values provide an approximate metal-proton distance. Bertini et al. demonstrated a clear

correlation for the [4Fe-4S] ferredoxins.[19—21] For example, protons close to the [4Fe-4S] cluster show very short T_1 values for HiPIPs[22,23] or Fds.[24] Assuming that the crystal structure of $[Fe_4S_4(SAr)_4]^{2-}$ is the same as the solution structure, the term $C[S(S+1)]f(\tau_c, \omega)$ can be fixed as a constant from both the crystal structure and the T_1 values of $[Fe_4S_4\{S\text{-}2,6\text{-}(CH_3CONH)_2C_6H_3\}_4]^{2-}$[4] as a standard. The distances among the Fe atom and the protons of the benzoyl group in **1** and **4** were evaluated from ^{1}H NMR T_1 experiments, as shown in Table 3. The signals assignable to 2′, 6′H (15 ms) and 3′, 5′H (52 ms) of the **4** indicate shorter T_1 values than those of **1** (22 and 84 ms). This result indicates that 2′, 6′H (4.6 Å) and 3′, 5′H (4.9 Å) of the benzoyl group in **4** are closer to the [4Fe-4S] cluster than those in **1** (4.9 and 6.1 Å, respectively).

Monte-Carlo simulations of **1** and **4** under ε=38 were performed in order to estimate the behavior of ligands in acetonitrile. The calculations for **1** and **4** at 300 K under ε=38 provide average Fe···H distances, as listed in Table 3. The distances obtained from a molecular-dynamics simulation show the same trend as the values estimated by using ^{1}H NMR T_1 experiments. The calculations of **4** give only one stable structure due to the bulkiness and coplanarity of 2,6-bis(benzoylamino)benzenethiolate, as shown in Fig. 2a. The protons 2′, 6′H (5.4 Å) of **4** are closer to the [4Fe-4S] cluster than that of **1** (7.0 Å) because the larger steric hindrance of the ligand 2,6-$(PhCONH)_2C_6H_3S^-$ restricts its conformation. In addition, the mean distance between 2′, 6′H of the benzoyl group and an inorganic sulfur atom in the cluster for **1** and **4** is estimated to be 4.3 and 6.2 Å, respectively (Fig. 2). Thus, the shorter C–H···S distance in a solution of **4**, estimated by using ^{1}H NMR T_1 values and a molecular simulation, suggests that the aromatic ring of the benzoyl group has a direct C–H···S interaction[16] with the inorganic sulfide of [4Fe-4S] cluster.

A Cooperative Positive Shift of the Redox Potential. The present model complexes exhibit a quasi-reversible redox couple of $[Fe_4S_4(SAr)_4]^{2-}/[Fe_4S_4(SAr)_4]^{3-}$ in acetonitrile at room temperature. The electrochemical data of these complexes, obtained from cyclic voltammography, are given in Table 4 and Fig. 3. The shift (Δ0.21—Δ0.25 V) observed for the benzoylamino-containing [4Fe-4S] complexes is larger than the value expected based on the number of NH···S hydrogen bonds (Fig. 3). Complex **1** gives a quasi-reversible

Table 4. Redox Potentials of $[Fe_4S_4(SAr)_4]^{2-/3-}$ in Acetonitrile at Room Temperature

Ar	$E_{1/2}$/V[a]	i_{pc}/i_{pa}
2-$PhCONHC_6H_4$ (**1**)	−0.86	1.0
2-(4-MeO-$C_6H_4CONH)C_6H_4$ (**2**)	−0.84	0.9
2-(4-F-$C_6H_4CONH)C_6H_4$ (**3**)	−0.82	0.9
2,6-$(PhCONH)_2C_6H_3$ (**4**)	−0.65	0.7
2,6-(4-MeO-$C_6H_4CONH)_2C_6H_3$ (**5**)	−0.63	0.7
2,6-(4-F-$C_6H_4CONH)_2C_6H_3$ (**6**)	−0.57	0.9
2-*t*-$BuCONHC_6H_4$[b]	−0.91	0.9
2,6-(*t*-$BuCONH)_2C_6H_3$[b]	−0.80	
2-*t*-BuCONH-6-PhC_6H_3[c]	−1.01	

a) V vs. SCE. b) Ref. 4. c) Ref. 14.

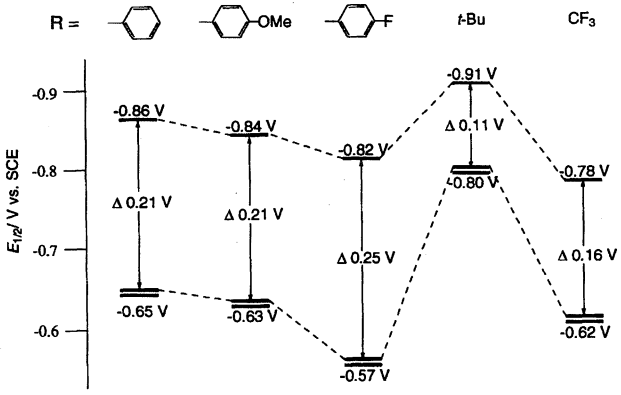

Fig. 3. Illustration of the redox potentials of $[Fe_4S_4(SAr)_4]^{2-/3-}$ and the differences between $[Fe_4S_4(S\text{-}2\text{-}RCONHC_6H_4)_4]^{2-}$ and $[Fe_4S_4\{S\text{-}2,6\text{-}(RCONH)_2C_6H_3\}_4]^{2-}$ in acetonitrile. Single and double bold lines indicate the redox potential of $[Fe_4S_4(S\text{-}2\text{-}RCONHC_6H_4)_4]^{2-/3-}$ and $[Fe_4S_4\{S\text{-}2,6\text{-}(RCONH)_2C_6H_3\}_4]^{2-/3-}$, respectively.

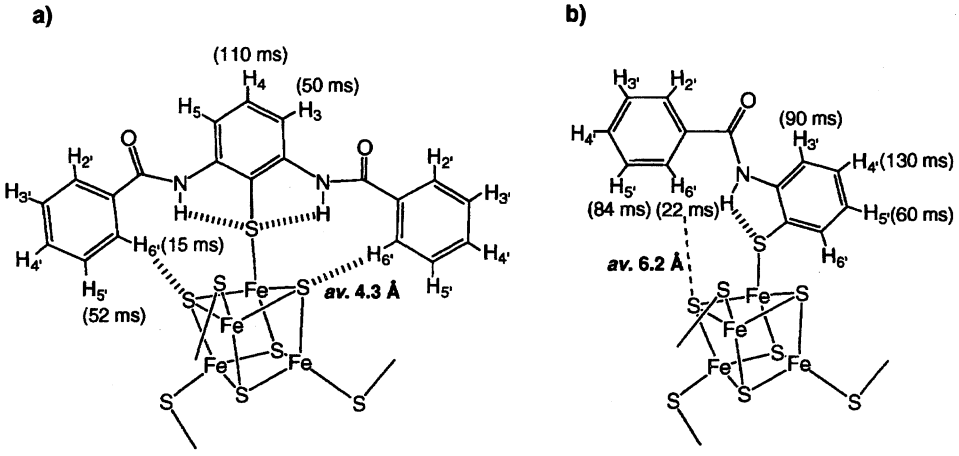

Fig. 2. Schematic drawing of proposed structures obtained from ^{1}H NMR T_1 analysis and MD calculation of a) **1** and b) **4**. ^{1}H NMR T_1 values are indicated in parentheses. The C–H···S distances in **1** and **4** are evaluated as averages from the MD calculations.

Table 5. The Correlation between Hammett Constants and the Redox Potentials of $[Fe_4S_4(SAr)_4]^{2-/3-}$ in Acetonitrile at 30 °C

X	$E_{1/2}$[a] of $[Fe_4S_4\{S\text{-}2\text{-}(4\text{-}X\text{-}C_6H_4CONH)C_6H_4\}_4]^{2-/3-}$	$E_{1/2}$[a] of $[Fe_4S_4\{S\text{-}2,6\text{-}(4\text{-}X\text{-}C_6H_4CONH)C_6H_4\}_4]^{2-/3-}$	σ_m	σ_p
H	−0.86	−0.65	0.00	0.00
OMe	−0.84	−0.63	0.12	−0.27
F	−0.82	−0.57	0.34	0.06

a) $E_{1/2}$/V vs. SCE.

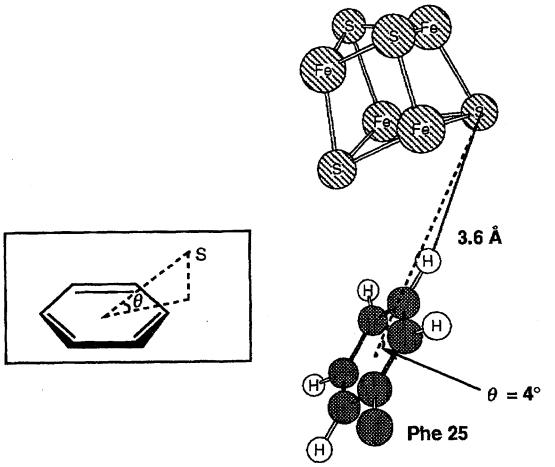

Fig. 4. Schematic drawing of the local structure of reduced FdI of Azotobacter vinelandii ferredoxin to show an approach of Phe 25 to the cluster. The data for drawing was obtained from Protein Data Bank (1FAD).[27]

redox couple of the 2−/3− species at −0.86 V vs. SCE (saturated calomel electrode) ($i_{p,c}/i_{p,a}$=1.0), whereas complex **4** indicates a similar redox couple at −0.65 V ($i_{p,c}/i_{p,a}$=0.7). The difference between the values for **1** and **4** is Δ0.21 V, which is too large, as judged from the number of NH···S hydrogen bonds. The differences between the values for **2** ($E_{1/2}$=−0.84 V) and **5** ($E_{1/2}$=−0.63 V), or **3** ($E_{1/2}$=−0.82 V) and **6** ($E_{1/2}$=−0.57 V) are Δ0.21 V or Δ0.25 V, respectively. The shift (Δ0.11 V) between mono- and bis(pivaloylamino) derivatives, $[Fe_4S_4(S\text{-}2\text{-}t\text{-}BuCONHC_6H_4)_4]^{2-}$ ($E_{1/2}$=−0.91 V) and $[Fe_4S_4\{S\text{-}2,6\text{-}(t\text{-}BuCONH)_2C_6H_3\}_4]^{2-}$ ($E_{1/2}$=−0.80 V), is considered to be the difference between singly and doubly NH···S hydrogen bonded complexes (Fig. 3). Previously, we reported on the regulation of the redox potential shift due to an electronic effect of an R group in RCONH of the arenethiolates. Even the difference between $[Fe_4S_4(S\text{-}2\text{-}CF_3CONHC_6H_4)_4]^{2-}$ ($E_{1/2}$=−0.78 V) and $[Fe_4S_4(S\text{-}2,6\text{-}(CF_3CONH)_2C_6H_3)_4]^{2-}$ ($E_{1/2}$=−0.62 V), both having an electron-withdrawing CF_3 group, is only Δ0.16 V.[4] Thus, the shifts between mono- and bis(benzoylamino)derivatives is not due to only an electronic effect of the benzoyl group.

Furthermore, the number of acylamino groups influences the pK_a values of the arenethiols, e.g. 2,6-$(PhCONH)_2C_6H_3SH$ and 2-$PhCONHC_6H_4SH$, 4.21 and 5.43, respectively. However, the pK_a values of the pivaloyl derivatives, 2,6-$(t\text{-}BuCONH)_2C_6H_3SH$ (pK_a=4.37) and 2-t-$BuCONHC_6H_4SH$ (pK_a=5.43) in an aqueous 10% $C_{12}H_{25}(OCH_2CH_2)_nOH$ micellar solution are similar. The difference in pK_a between the bis(acylamino) derivatives, e.g. 2,6-$(t\text{-}BuCONH)_2C_6H_3SH$ and 2,6-$(PhCONH)_2C_6H_3SH$ is only 0.16 pK_a unit. Therefore, the large positive shift of the redox potentials for **4**—**6** is caused by the participation of the aromatic ring of the benzoyl group.

The direct interaction of the aromatic ring was also investigated based on the dependence of the redox potential on *p*-substituents of the aromatic ring of the benzoyl. Three different mono-substituted compounds (OMe, H, F) were studied. Table 5 lists the redox potentials of **4**—**6** to show the correlation between the redox potential and Hammett σ_m or σ_p values. If the redox potentials of **4**—**6** depend only on the strength of the NH···S hydrogen bond, a good correlation between the Hammett σ_p constants and the redox potential could be obtained. Already, the distal *para* substituent effects through the NH···S hydrogen bonds on the positive shift of the redox potential of $[Fe_4S_4(Z\text{-}cys\text{-}Gly\text{-}NHC_6H_4\text{-}p\text{-}X)_4]^{2-/3-}$ have been demonstrated to show a good correlation with the Hammett σ_p constants.[9]

Our present results clearly indicate a reasonable correlation with the Hammett σ_m values, but not with the Hammett σ_p. The C–H···S interaction between benzoyl *m*-H and inorganic sulfide, estimated by using both the ^{1}H NMR T_1 experiment and molecular dynamics, is thus thought to contribute to the positive shift of the $[Fe_4S_4(SAr)_4]^{3-}/[Fe_4S_4(SAr)_4]^{2-}$ redox couple.

Previously, we reported another type of aromatic interaction for a [4Fe-4S] complex having a single NH···S hydrogen bond and an aromatic group, $[Fe_4S_4(S\text{-}2\text{-}t\text{-}BuCONH\text{-}6\text{-}PhC_6H_3)_4]^{2-}$.[14] In this case, the coexistence of an aromatic ring and a NH···S hydrogen bond contributes to the stabilization of the $[Fe_4S_4(SAr)_4]^{1-}/[Fe_4S_4(SAr)_4]^{2-}$ redox couple. However, complexes **4**—**6** exhibit irreversible $[Fe_4S_4(SAr)_4]^{1-}/[Fe_4S_4(SAr)_4]^{2-}$ redox couples in acetonitrile. Therefore, the phenyl ring of $[Fe_4S_4(S\text{-}2\text{-}t\text{-}BuCONH\text{-}6\text{-}PhC_6H_3)_4]^{2-}$ probably stacks over the sulfur atom, thus making a difference from the cases of **4**—**6**.[14]

In conclusion, the proximal *m*-H of benzoyl ring in **4** makes contacts with an inorganic sulfur atom, as concluded from an ^{1}H NMR T_1 analysis and molecular-dynamics simulations. It is likely that the C–H···S interaction between a positively charged benzoyl *m*-H and an inorganic sulfur atom for complex **4**—**6** contributes the positive shift of the $[Fe_4S_4(SAr)_4]^{3-}/[Fe_4S_4(SAr)_4]^{2-}$ redox potential. Among native [4Fe-4S] ferredoxins, two structural data (1), a short distance (3.6 Å) of the C–H···S and (2) a small angle (4°) be-

tween the centroid of aromatic ring and the inorganic sulfur atom of [4Fe-4S] cluster, were reported for reduced *A. v.* Fd, as shown in Fig. 4. Our model study strongly suggests that the C–H···S interaction regulates the redox potential with the specific orientation of the proximal aromatic plane in the active center of native [4Fe-4S] ferredoxins.

Experimental

All procedures were performed in an argon atmosphere by the Schlenk technique. All of the solvents were dried over calcium hydride and distilled under argon before use.

Preparation of Bis(2-benzoylaminophenyl) Disulfide. To a dry THF solution (30 cm^3) of bis(2-aminophenyl) disulfide (1.0 g, 4.0 mmol) was added triethylamine (1.3 cm^3, 9.4 mmol), then, benzoyl chloride (1.0 cm^3, 8.7 mmol) was added dropwise with vigorous stirring in an ice-water bath for 1 h at room temperature overnight. The solution was poured over ice and water, to give a pale-yellow powder as a precipitate. The powder was dissolved in diethyl ether (200 cm^3), and ether layer was successively washed with a 2% aqueous HCl solution, water, a 4% aqueous $NaHCO_3$ solution, and water. Then pale-yellow crystals were precipitated from the organic layer. The organic layer was dried over anhydrous sodium sulfate and concentrated under reduced pressure to give pale-yellow crystals, which were crystallized from THF. The pale-yellow materials were dried over P_2O_5. Yield 1.7 g (90%). ^{1}H NMR (DMSO-d_6) δ=7.34 (m, 6H), 7.59 (m, 8H), 7.97 (d, 4H), and 10.26 (s, 2H). Found: C, 68.27; H, 4.32; N, 6.17%. Calcd for $C_{26}H_{20}N_2O_2S_2$: C, 68.40; H, 4.42; N, 6.14%.

Preparation of Bis[2,6-bis(benzoylamino)phenyl] Disulfide. The compound was synthesized from a 1,4-dioxane solution (30 cm^3) of bis(2,6-diaminophenyl) disulfide (0.28 mg, 1.0 mmol) and pyridine (0.8 cm^3, 10 mmol) by the same method as described for bis(2-benzoylaminophenyl) disulfide. The extracted organic layer was dried over anhydrous sodium sulfate and concentrated under reduced pressure to give a red oil. The crude oil was reprecipitated from THF and hexane. The yellow-brown materials obtained were dried over P_2O_5. Yield 280 mg (40%). ^{1}H NMR (DMSO-d_6) δ=7.23 (t, 2H), 7.49 (t, 8H), 7.59 (d, 4H), 7.66 (d, 4H), 7.73 (d, 8H), and 9.70 (s, 4H). Found: C, 68.34; H, 4.29; N, 8.10%. Calcd for $C_{40}H_{30}N_4O_4S_2$: C, 69.14; H, 4.35; N, 8.06%.

Preparation of Bis[2-(4-anisoylamino)phenyl] Disulfide. The compound was synthesized by the same method as described for bis(2-benzoylaminophenyl) disulfide. Pale-yellow needles crystallized from THF and diethyl ether were dried over P_2O_5. Yield 1.56 g (75%). ^{1}H NMR (DMSO-d_6) δ=3.84 (s, 6H), 7.06 (d, 4H), 7.25 (t, 2H), 7.28 (t, 2H), 7.36 (t, 2H), 7.64 (d, 2H), 7.95 (d, 4H), and 10.09 (s, 2H). Found: C, 64.77; H, 4.62; N, 5.37%. Calcd for $C_{28}H_{24}N_2O_4S_2$: C, 65.10; H, 4.68; N, 5.42%.

Preparation of Bis[2-(4-fluorobenzoylamino)phenyl] Disulfide. The compound was prepared using the same method as described for bis(2-benzoylaminophenyl) disulfide. Pale-yellow microcrystals were obtained by reprecipitation from THF and hexane. The yellow crystals were dried over P_2O_5. Yield 1.71 g (83%). ^{1}H NMR (DMSO-d_6) δ=7.36 (m, 10H), 7.65 (d, 2H), 8.04 (m, 4H), and 10.28 (s, 2H). Found: C, 63.43; H, 3.65; N, 5.69%. Calcd for $C_{26}H_{18}F_2N_2O_2S_2$: C, 63.40; H, 3.68; N, 5.69%.

Preparation of Bis[2,6-di(4-anisoylamino)phenyl] Disulfide. The compound was synthesized by the same method in dry THF as described for bis[2,6-bis(benzoylamino)phenyl] disulfide. Yellow materials were dried over P_2O_5. Yield 701 mg (73%). ^{1}H NMR (DMSO-d_6) δ=3.85 (s, 12H), 7.00 (d, 8H), 7.23 (t, 2H), 7.65 (d, 4H), 7.70 (d, 8H), and 9.51 (s, 4H). Found: C, 64.35; H, 4.68; N, 7.02%. Calcd for $C_{44}H_{38}N_4O_8S_2$: C, 64.85; H, 4.70; N, 6.87%.

Preparation of Bis[2,6-di(4-fluorobenzoylamino)phenyl] Disulfide. The compound was prepared using the same method as described for bis[2,6-bis(4-anisoylamino)phenyl] disulfide. Yield 0.60 g (66%). ^{1}H NMR (DMSO-d_6) δ=7.21 (t, 2H), 7.31 (m, 8H), 7.59 (d, 4H), 7.80 (m, 8H), and 9.73 (s, 4H). Found: C, 62.08; H, 3.39; N, 7.47%. Calcd for $C_{40}H_{26}F_4N_4O_4S_2$: C, 62.66; H, 3.42; N, 7.31%.

Synthesis of $(Et_4N)_2[Fe_4S_4(S\text{-}2\text{-}PhCONHC_6H_4)_4]$ (1). The complex was synthesized by a ligand-exchange method.[4] A mixture of $(Et_4N)_2[Fe_4S_4(SPh)_4]$[10] (53 mg, 0.05 mmol) and bis(2-benzoylaminophenyl) disulfide (49 mg, 0.11 mmol) in acetonitrile (5 cm^3) was stirred at room temperature overnight. The solution was concentrated under reduced pressure. A black crude product was washed with diethyl ether and reprecipitated from acetonitrile/diethyl ether; and a black oil was obtained, and dried in vacuo. The yield was 81%. UV (CH_3CN) 300 nm (ε 37000), 388 (sh, 19000), and 456 (sh, 14000); MS (FAB) *m/z* 1394. Calcd for $\{(Et_4N)[Fe_4S_4(S\text{-}2\text{-}PhCONHC_6H_4)_4]\}^-$: 1393.98. Found: C, 52.39; H, 5.24; N, 5.24%. Calcd for $C_{68}H_{80}Fe_4N_6O_4S_8$: C, 53.55; H, 5.29; N, 5.51%.

Syntheses of $(Et_4N)_2[Fe_4S_4(SAr)_4]$ {Ar=2-(4-MeO-C_6H_4-CONH)C_6H_4 (2), 2-(4-F-C_6H_4CONH)C_6H_4 (3), 2,6-$(PhCONH)_2C_6H_3$ (4), 2,6-(4-MeO-C_6H_4CONH)$_2C_6H_3$ (5), and 2,6-(4-F-C_6H_4CONH)$_2C_6H_3$ (6)}. These complexes were synthesized by a similar method as that for **1**, and were obtained as a brownish powder.

$(Et_4N)_2[Fe_4S_4\{S\text{-}2\text{-}(4\text{-}MeO\text{-}C_6H_4CONH)C_6H_4\}_4]$ (2): The yield was 78%. UV (CH_3CN) 380 (sh, 19000) and 458 (sh, 15000); MS (FAB) *m/z* 1384. Calcd for $[Fe_4S_4\{S\text{-}2\text{-}(4\text{-}MeO\text{-}C_6H_4CONH)\text{-}C_6H_4\}_4]^-$: 1383.86. Found: C, 51.64; H, 5.35; N. 5.16%. Calcd for $C_{72}H_{88}Fe_4N_6O_8S_8$: C, 52.56; H, 5.39; N, 5.11%.

$(Et_4N)_2[Fe_4S_4\{S\text{-}2\text{-}(4\text{-}F\text{-}C_6H_4CONH)C_6H_4\}_4]$ (3): The yield was 92%. Found: C, 50.03; H, 4.80; N, 5.18%. Calcd for $C_{68}H_{76}F_4Fe_4N_6O_4S_8$: C, 51.13; H, 4.80; N, 5.26%. UV (CH_3CN) 387 (sh, 18000) and 455 (sh, 14000), MS (FAB) *m/z* 1466. Calcd for $\{(Et_4N)[Fe_4S_4\{S\text{-}2\text{-}(4\text{-}F\text{-}C_6H_4CONH)C_6H_4\}_4]\}^-$: 1465.94.

$(Et_4N)_2[Fe_4S_4\{S\text{-}2,6\text{-}(PhCONH)_2C_6H_3\}_4]$ (4): The yield was 93%. UV (CH_3CN) 368 (21000) and 466 (sh, 12000); MS (FAB) *m/z* 1871. Calcd for $\{(Et_4N)[Fe_4S_4\{S\text{-}2,6\text{-}(PhCONH)_2C_6H_3\}_4]\}^-$: 1870.13. Found: C, 55.00; H, 4.91; N, 6.69%. Calcd for $C_{96}H_{100}Fe_4N_{10}O_8S_8$: C, 57.60; H, 5.04; N, 7.00%.

$(Et_4N)_2[Fe_4S_4\{S\text{-}2,6\text{-}(4\text{-}MeO\text{-}C_6H_4CONH)_2C_6H_3\}_4]$ (5): The yield was 87%. UV (CH_3CN) 377 (sh, 22000) and 466 (sh, 16000); MS (FAB) *m/z* 1981. Calcd for $\{[Fe_4S_4\{S\text{-}2,6\text{-}(4\text{-}MeO\text{-}C_6H_4CONH)_2C_6H_3\}_4]^{2-}+H^+\}^-$: 1981.05. Found: C, 54.63; H, 5.15; N, 6.30%. Calcd for $C_{104}H_{116}Fe_4N_{10}O_{16}S_8$: C, 55.71; H, 5.21; N, 6.25%.

$(Et_4N)_2[Fe_4S_4\{S\text{-}2,6\text{-}(4\text{-}F\text{-}C_6H_4CONH)_2C_6H_3\}_4]$ (6): The yield was 88%. UV (CH_3CN) 377 (sh, 20000) and 467 (sh, 14000); MS (FAB) *m/z* 1885. Calcd for $\{[Fe_4S_4\{S\text{-}2,6\text{-}(4\text{-}F\text{-}C_6H_4CONH)_2C_6H_3\}_4]^{2-}+H^+\}^-$: 1884.89. Found: C, 53.17; H, 4.25; N, 6.60%. Calcd for $C_{96}H_{92}F_8Fe_4N_{10}O_8S_8$: C, 53.74; H, 4.32; N, 6.53%.

Physical Measurements. The absorption spectra were recorded using a JASCO Ubest-30 spectrometer or a Shimadzu UV-3100PC spectrometer in units of M^{-1} cm^{-1} (1 M=1 mol dm^{-3}). An IR spectrum measurement in the solid state was performed on a JASCO FT/IR-8300 spectrometer. Samples were prepared as KBr pellets. The ^{1}H NMR spectra were measured on a JEOL JNM-EX 270 MHz FT NMR spectrometer. Tetramethylsilane (TMS) was

used as an external reference in the ^{1}H NMR spectra. The T_1 values of the ^{1}H NMR signals were obtained by an inversion recovery method using a 180°-τ-90° pulse. with a delay between 180° and 90° pulses. Measurements of cyclic voltammograms in an acetonitrile solution were carried out on a BAS100B CV-100W instrument with a three-electrode system: a glassy carbon working electrode, a Pt-wire auxiliary electrode and a saturated calomel electrode (SCE). The scan rate was 100 mV s^{-1}. The sample concentration was about 2.5 mM, containing 0.1 M of n-Bu_4NClO_4 as a supporting electrolyte. The potentials were determined at room temperature vs. SCE as a reference. A mass-spectrometric analysis was performed in a solution with a matrix (NBA=3-nitrobenzyl alcohol) on a JEOL JMS-SX102 mass spectrometer, which was operated in a negative-ion mode. Ions were produced by fast-atom bombardment (FAB) with a beam of 3 keV Xe atoms, and an accelerating voltage of 10 kV.

Molecular Dynamics Calculations. The Monte-Carlo and molecular-dynamics simulations were carried out using a Biograf ver 3.22 (Molecular Simulation Inc. 1992). A Dreiding force field was employed for the calculations.[25] The charge of each atom was readjusted stepwise using a charge-equilibration method.[26] The calculations of $[Fe_4S_4(SAr)_4]^{2-}$ were carried out using both bonded and nonbonded terms. The Fe ions of $[Fe_4S_4]^{2+}$ core were constrained to a tetrahedral geometry.

We are grateful for financial support from the JSPS Fellowships (Takafumi Ueno.; No. 2691, 1995—1998) for Japanese Junior Scientists and for a Grant-in-Aid for Specially Promoted Research (Akira Nakamura; No. 06101004) from the Ministry of Education, Science and Culture.

References

1) A. Nakamura and N. Ueyama, "Encyclopedia of Inorganic Chemistry," ed by R. B. King, John Wiley & Sons, New York (1994), Vol. 4, pp. 1883—1896.

2) M. K. Johnson, "Encyclopedia of Inorganic Chemistry," ed by R. B. King, John Wiley & Sons, New York (1994), Vol. 4, pp. 1896—1915.

3) C. W. Carter, *J. Biol. Chem.*, **252**, 7802 (1977).

4) N. Ueyama, Y. Yamada, T. Okamura, S. Kimura, and A. Nakamura, *Inorg. Chem.*, **35**, 6473 (1996).

5) N. Ueyama, T. Okamura, and A. Nakamura, *J. Am. Chem. Soc.*, **114**, 8129 (1992).

6) N. Ueyama, T. Okamura, M. Nakata, and A. Nakamura, *J. Am. Chem. Soc.*, **105**, 7098 (1983).

7) K. Fukuyama, H. Matsubara, T. Tukihara, and Y. Katube, *J. Mol. Biol.*, **210**, 383 (1989).

8) I. Rayment, G. Wesenberg, T. E. Meyer, M. A. Cusanovich, and H. M. Holden, *J. Mol. Biol.*, **228**, 672 (1992).

9) R. Ohno, N. Ueyama, and A. Nakamura, *Inorg. Chem.*, **30**, 4877 and 4891 (1991).

10) B. V. DePamphilis, B. A. Averill, T. Herskovitz, J. L. Que, and R. H. Holm, *J. Am. Chem. Soc.*, **96**, 4159 (1974).

11) R. H. Holm, W. D. Phillips, B. A. Averill, J. J. Mayerle, and T. Herskovitz, *J. Am. Chem. Soc.*, **96**, 2109 (1974).

12) R. Krishnamoorthi, J. L. Markley, M. A. Cusanovich, C. T. Przysiecki, and T. E. Meyer, *Biochemistry*, **25**, 60 (1986).

13) S. M. Lui and J. A. Cowan, *J. Am. Chem. Soc.*, **116**, 4483 (1994).

14) T. Ueno, N. Ueyama, and A. Nakamura, *J. Chem. Soc., Dalton Trans.*, **1996**, 3859.

15) R. S. Morgan, C. E. Tatsch, R. H. Gushard, J. M. McAdon, and P. K. Warme, *Int. J. Peptide Protein Res.*, **11**, 209 (1978).

16) K. S. C. Reid, P. F. Lindley, and J. M. Thornton, *FEBS Lett.*, **190**, 209 (1985).

17) N. Ueyama, T. Okamura, Y. Yamada, and A. Nakamura, *J. Org. Chem.*, **60**, 4893 (1995).

18) I. Solomon, *Phys. Rev.*, **99**, 559 (1955).

19) I. Bertini, A. Donaire, B. A. Feinberg, C. Luchinat, M. Piccioli, and H. Yuan, *Eur. J. Biochem.*, **232**, 192 (1995).

20) I. Bertini, F. Briganti, C. Luchinat, and A. Scozzafava, *Inorg. Chem.*, **29**, 1874 (1990).

21) I. Bertini, F. Briganti, C. Luchinat, L. Messori, R. Monnanni, A. Scozzafava, and G. Vallini, *FEBS Lett.*, **289**, 253 (1991).

22) L. Banci, I. Bertini, S. Ciurli, S. Ferretti, C. Luchinat, and M. Piccioli, *J. Am. Chem. Soc.*, **32**, 9387 (1993).

23) H. Rüterjans, L. Messori, O. Ohlenschläger, F. Briganti, and I. Bertini, *Appl. Magn. Reson.*, **4**, 477 (1993).

24) S. C. Busse, G. N. L. Mar, L. P. Yu, J. B. Howard, E. T. Smith, Z. H. Zhou, and M. W. W. Adams, *Biochemistry*, **31**, 11952 (1992).

25) S. L. Mayo, B. D. Olafson, and W. A. Goddard, III, *J. Phys. Chem.*, **94**, 8897 (1990).

26) A. K. Rappe and W. A. Goddard, III, *J. Phys. Chem.*, **95**, 3358 (1991).

27) This was obtained from Brookhaven Protein Data Bank. This data bank file name is 1FAD (C. D. Stout et al., 1993).